MASTER

ORNL-3117
UC-4 – Chemistry

INTERDIFFUSION OF HELIUM AND ARGON IN SPEER MODERATOR NO. 1 GRAPHITE

(A Terminal Report on Large-Pore Graphites – Experimental Phase)

Jack Truitt

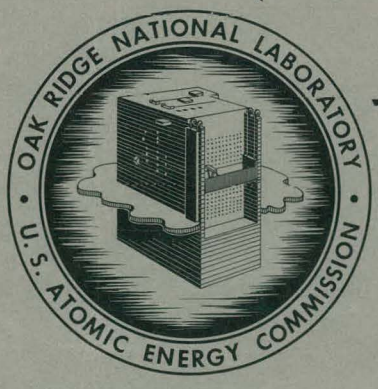

OAK RIDGE NATIONAL LABORATORY
operated by
UNION CARBIDE CORPORATION
for the
U.S. ATOMIC ENERGY COMMISSION

DISCLAIMER

ORNL-3117

Contract No. W-7405-eng-26

REACTOR CHEMISTRY DIVISION

INTERDIFFUSION OF HELIUM AND ARGON IN SPEER MODERATOR NO. 1 GRAPHITE
(A Terminal Report on Large-Pore Graphites – Experimental Phase)

Jack Truitt

DATE ISSUED

JUN 26 1961

OAK RIDGE NATIONAL LABORATORY
Oak Ridge, Tennessee
operated by
UNION CARBIDE CORPORATION
for the
U.S. ATOMIC ENERGY COMMISSION

THIS PAGE

WAS INTENTIONALLY

LEFT BLANK

CONTENTS

INTERDIFFUSION OF HELIUM AND ARGON IN SPEER MODERATOR NO. 1 GRAPHITE
(A Terminal Report on Large-Pore Graphites – Experimental Phase)

Jack Truitt

ABSTRACT

Design studies of high-temperature gas-cooled reactors have shown the necessity of minimizing coolant contamination by radioactive fission products and corrosive gases. One proposed method – use of a critical sweep rate of the helium coolant to oppose diffusion of undesirable gases into the coolant stream – requires knowledge of the back-diffusion of these gases against a stream of helium flowing through small cracks and porous media. Although the material studied (high-permeability graphite) was not of the type which would actually be employed in a reactor the flow mechanisms studied should occur in the less permeable materials at very high pressure. Thus these studies should be of value with respect to the problem outlined above.

An experimental investigation of the interdiffusion and forced-flow behavior of helium and argon in Speer Moderator No. 1 was performed. These data were employed to determine a mutual diffusion coefficient and to verify certain superposed-flow equations. In addition, two series of experiments at high values of the forced-flow component were conducted to investigate contributions of the back-diffusion mechanism of those pores whose diameters are equal to or smaller than the mean free path of the gas molecules (approaching Knudsen or free-molecule diffusion).

At small forced-flow rates, normal diffusion was the controlling diffusion mechanism, while Knudsen effects were negligible. Flow equations employed previously are applicable to these data.

Experiments conducted at high forced-flow rates show the contribution of small channels. This contribution appears to follow the Knudsen diffusion mechanism. A critical value of sweep rate was determined experimentally. If the sweep rate is lower than the critical, the contamination will increase, whereas sweep rates greater than this would require large reprocessing capacities without additional decrease in contamination.

Structural changes in the graphite due to fission of the UO_2-graphite fuel were not considered in this study of the basic mechanisms of interdiffusion. These would include pore-size changes or the possible increase

of surface effects due to fission-product deposition on pore channel walls and the presence of more active gases.

INTRODUCTION

The proposed use of a coolant gas sweep stream to oppose diffusion of radioactive and corrosive gases into the coolant system[1] has inspired a study of the interdiffusion and forced-flow behavior of helium and argon in Speer Moderator No. 1 graphite.

Previous diffusion experiments[2] with AGOT graphite resulted in a single normalized mutual-diffusion coefficient and indicated that the classical diffusion mechanism was controlling with a negligible amount of surface and Knudsen diffusion. A net drift effect was observed. The ratio of the helium diffusion rate to that of argon was inversely proportional to the square root of the ratio of the atomic weights of the two gases. The value of the mutual diffusion coefficient was independent of the value of forced-flow rate. Comparisons of experimental data obtained from combined forced and diffusive flow with predicted values (calculations based on average permeability values and the mutual diffusion coefficient for helium-argon mixtures) demonstrated that accurate estimates of combined flow could be made. A slightly lower permeability graphite (Speer Moderator No. 1) was selected to continue and expand the scope of the previous diffusion studies.

This investigation involved the determination of mutual diffusion coefficients for the binary gas mixture and a permeability coefficient for the individual gases and known mixture. Next, rates of diffusion superposed on forced flow were determined and compared with the predicted values.

---

[1]W. B. Cottrell et al., A Design Study of a Nuclear Power Station Employing a High-Temperature Gas-Cooled Reactor with Graphite-UO_2 Fuel Elements, ORNL-2653 (July 14, 1959).

[2]R. B. Evans III, J. Truitt, and G. M. Watson, Interdiffusion of Helium and Argon in a Large-Pore Graphite, ORNL CF-60-11-102 (Nov. 23, 1960).

Several experiments were performed to ascertain the effects on the system which would result from utilizing mixtures as the test gas. Finally, a series of experiments were made to test the validity of present postulated flow equations at high sweep rates.

Essentially this is two reports: an academic study of diffusion calculations and mechanisms, and one on experiments applicable to the coolant contamination problem. They are combined in order to show the purpose and direction of the theoretical work and to illustrate both the desirability and the difficulty of arriving at physical interpretations of certain suggestive factors that appear in the equations and plotted data. Of particular interest is the appearance of "crossover" points (where the vectors corresponding to flow components reverse direction).

The experimental (but not the theoretical) phase of the work with large-pore graphites is closed. Further experiments will be with small-pore graphite.

MATERIALS AND PROCEDURES

Nomenclature

A	Cross sectional area normal to flow, cm^2
D_{12}	Mutual diffusion coefficient, cm^2/sec
D_K	Knudsen diffusion coefficient, cm^2/sec
D_o	Normalized mutual diffusion coefficient, cm^2/sec
K	Permeability coefficient, cm^2/sec
k_o	Permeability constant at infinite pressure, darcy or cm^2
L	Length along path of flow, cm
M	Molecular or atomic weight, g/mole
$\dot{n}_{Ar}$	Total argon flow rate, mole/sec
$\dot{n}_f$	Forced-flow rate, mole/sec
$\dot{n}_{He}$	Total helium flow rate, mole/sec
$\dot{n}_T$	Net flow rate, mole/sec
$\dot{n}_T'$	Net diffusive flow at uniform pressure, mole/sec
N_{Ar}	Mole fraction of argon at point x
N_{He}	Mole fraction of helium at point x
P	Total pressure, $dyne/cm^2$ or atm

P_m Mean flowing pressure, dyne/cm^2 or atm

R Gas constant, 82.05 cm^3-atm/mole °K

T Temperature, °K

x Variable position along L, cm

z Radial thickness factor

ζ_{12} Total diffusive driving force, mole/cm^4

ΔP Pressure drop along L, dyne/cm^2 or atm

Materials

The porous medium utilized for all the experiments covered by this report was Speer Moderator No. 1 graphite (manufactured by Speer Carbon Co., Saint Marys, Penn.). This material has the same general flow-governing qualities as AGOT. Characterization data are shown below.

Characteristics	Speer Moderator No. 1	AGOT
k_0, 20°C, $1/P_m \rightarrow 0$ millidarcy	10	21
Porosity based on helium absorption vol %	17.8 (ref 3)	22
Total porosity based on 2.25 g/cc	23.2	26

Cylinders of analyzed helium and argon were used as the sources of gas for the experiments. The free oxygen content of these gases ranged from 1 to 4 ppm. The water concentrations, determined by a dew-point method, were 10 to 15 ppm. No attempts at additional purification were made.

Experimental Procedure

The diffusion cell employed in these experiments was identical to those used previously.[4] The septum was in the form of a thin-walled cylinder closed at both ends. Helium (or a helium-argon mixture) was swept

[3] J. Truitt et al., Transport of Gases Through Ceramic Material, ORNL-2931, p 153.

[4] R. B. Evans III, J. Truitt, and G. M. Watson, Superposition of Forced and Diffusive Flow in a Large-Pore Graphite, ORNL-3067 (Jan. 17, 1961).

past the inner face; argon was swept along the outer face. The diffusion rates were measured by analyzing the contamination of the effluent gas streams. This was possible since the gases were pure (or known mixtures). Total pressure drop across the septum was measured by means of a butyl phthalate manometer. All pressures, pressure drops, temperatures, and flow rates were measured with suitable devices which were properly calibrated. Detailed description of the apparatus may be found elsewhere.[4] One significant change was made in the procedure: the majority of the gas analyses were performed with the thermal-conductivity cells. A mass spectrometer was employed on previous experiments. Previous experiments had demonstrated that small pressure drops across the graphite would not affect the determination of a mutual diffusion coefficient; therefore final pressure-drop calibrations were ascertained after termination of the diffusion experiments.

These pressure-drop corrections were made in calculating permeability constants and diffusion coefficients.

RESULTS

Forced-Flow Experiments

Helium, argon, and helium-argon mixture permeability determinations[5] were made on the diffusion cell before, during, and after completion of the diffusion experiments in order to determine whether the septum characteristics remained constant. These data are shown on Fig. 1 and Tables 1, 2, and 3.

Since permeability constants can be evaluated only in the viscous-flow region, considerable care was taken to ensure that the measurements were obtained in this region. The dotted curves of Fig. 1 show typical turbulent-flow data. The solid curves correspond to viscous-flow data. The agreement between determinations performed at different stages of the experiments demonstrates that the septum characteristics were constant during the entire series of diffusion experiments. Contributions resulting from Knudsen effects are small, as reflected by the low intercept

---

[5] "Standard Procedure for Determining Permeability of Porous Media," API Code No. 27, 2nd ed., American Petroleum Institute, Division of Production, Dallas, Texas, 1942.

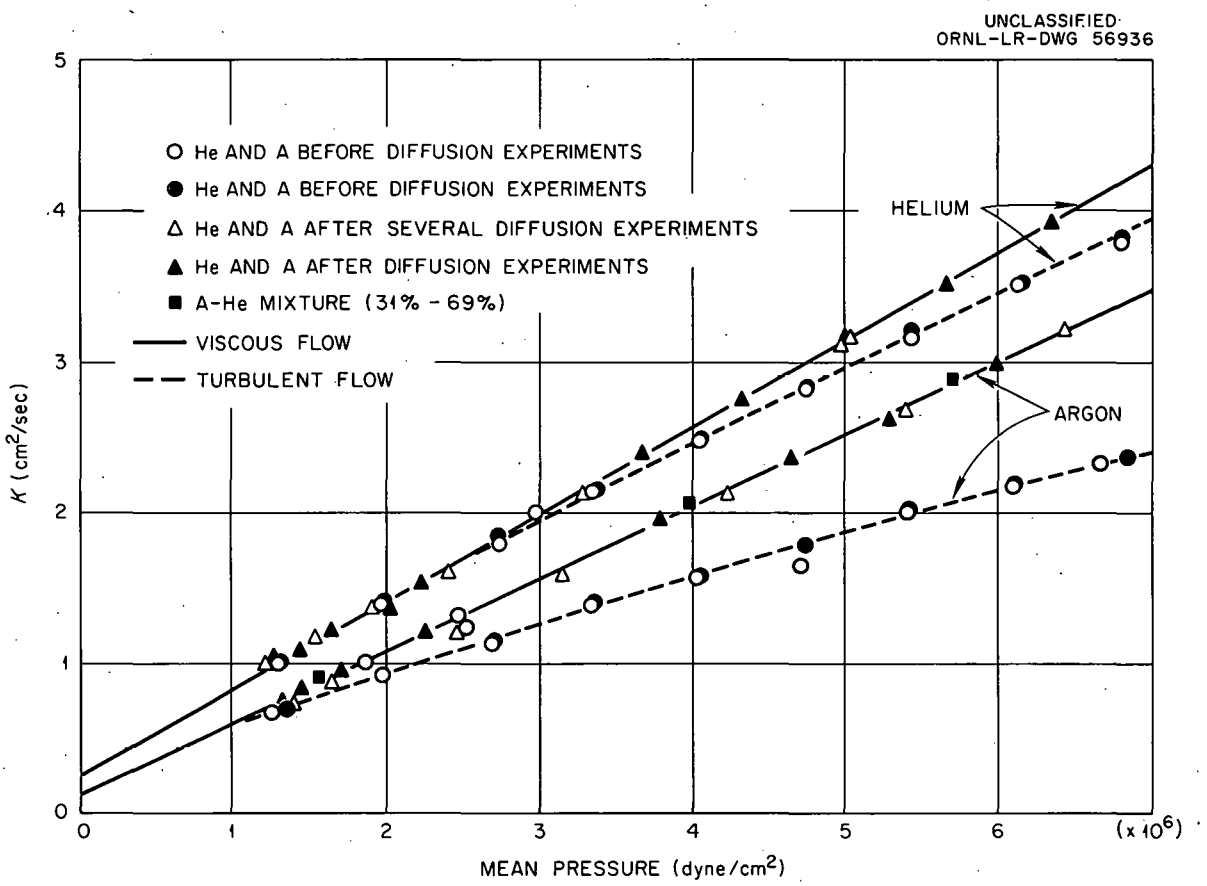

Fig. 1. Permeability Data for Speer No. 1 Graphite Diffusion Cell.

Table 1. Permeability Data of Graphite Diffusion Cell to Helium

(Speer Carbon Co. Moderator No. 1 Grade)

Series A Before diffusion determinations (ΔP = 202 mm Hg)
Series B Before diffusion determinations (ΔP = 202 mm Hg)
Series C During diffusion determinations (ΔP = 36.8 mm Hg)
Series D After diffusion experiments termination (ΔP = 27.4 mm Hg)

Series A		Series B		Series C		Series D	
P_m* (dyne/cm^2)	$K_{20°C}$** (cm^2/sec)	P_m (dyne/cm^2)	$K_{20°C}$ (cm^2/sec)	P_m (dyne/cm^2)	$K_{20°C}$ (cm^2/sec)	P_m (dyne/cm^2)	$K_{20°C}$ (cm^2/sec)
7.51	4.12	7.53	4.17	5.03	3.14	6.35	3.92
6.81	3.80	6.84	3.86	4.99	3.08	5.64	3.52
6.13	3.50	6.15	3.49	3.34	2.13	4.98	3.14
5.44	3.16	5.46	3.22	2.40	1.59	4.31	2.76
4.75	2.80	4.77	2.85	2.01	1.37	3.68	2.40
4.06	2.46	4.08	2.49	1.64	1.17	2.97	2.00
3.37	2.11	3.39	2.13	1.48	1.05	2.22	1.53
2.72	1.79	2.70	1.76	1.32	0.97	1.91	1.36
1.99	1.38	2.01	1.40			1.66	1.21
1.30	0.99	1.32	0.99			1.47	1.09
						1.29	0.98

*Mean flowing pressure (dyne/cm^2 $\times$ 10^6).
**Permeability coefficient.

Table 2. Permeability Data of Graphite Diffusion Cell to Argon

(Speer Carbon Co. Moderator No. 1 Grade)

Series A Before diffusion determinations (ΔP = 202 mm Hg)
Series B Before diffusion determinations (ΔP = 202 mm Hg)
Series C During diffusion determinations (ΔP = 36.9 mm Hg)
Series D After diffusion experiments termination (ΔP = 28.7 mm Hg)

Series A		Series B		Series C		Series D	
P_m* (dyne/cm^2)	$K_{20°C}$** (cm^2/sec)	P_m (dyne/cm^2)	$K_{20°C}$ (cm^2/sec)	P_m (dyne/cm^2)	$K_{20°C}$ (cm^2/sec)	P_m (dyne/cm^2)	$K_{20°C}$ (cm^2/sec)
7.49	2.49	7.54	2.55	6.46	3.20	5.98	2.95
6.79	2.32	6.84	2.36	5.40	2.66	5.30	2.60
6.11	2.15	6.15	2.19	4.26	2.06	4.65	2.35
5.42	1.97	5.46	2.00	3.16	1.55	3.80	1.94
4.72	1.63	4.77	1.80	2.44	1.26	2.50	1.34
4.04	1.57	4.09	1.60	1.66	0.88	2.26	1.22
3.35	1.37	3.40	1.37	1.42	0.78	1.87	1.01
2.70	1.14	2.71	1.16			1.70	0.93
1.97	0.91	2.03	0.91			1.46	0.81
1.28	0.66	1.34	0.67			1.31	0.75

*Mean flowing pressure (dyne/cm^2 $\times$ 10^6).
**Permeability coefficient.

Table 3. Permeability Data of Graphite Diffusion Cell to 69% Helium–31% Argon Mixture

(Speer Carbon Co. Moderator No. 1 Grade)

After termination of diffusion experiments

ΔP = 30.0 mm Hg

P_m (dyne/cm^2)	$K_{20°C}$ (cm^2/sec)
5.70×10^6	2.88
3.96×10^6	2.05
2.44×10^6	1.30
1.57×10^6	0.91

values of Fig. 1. All permeability constants were correlated on the basis of established viscosity data.[6] These data were employed in correlating the results of subsequent superposed-flow experiments.

Diffusion Experiments

Correlation of Diffusion Data

The following equation[4] was used to obtain D_{12} from the experimental data:

$$\dot{n}_T = D_{12} \frac{A}{L} \frac{P}{RT} \ln \left[\frac{\dot{n}_{He} - \dot{n}_T N_{He}(L)}{\dot{n}_{He} - \dot{n}_T N_{He}(0)} \right] , \qquad (1)$$

where the helium concentration at the surfaces x = 0 and x = L has been inserted. Equation (1) is derived from the following basic equations:

$$\dot{n}_1 = N_1 \dot{n}_T - D_{12} A \frac{P}{RT} \frac{dN_1}{dx} , \qquad (2)$$

$$D_{12} \frac{dN_1}{dx} = -D_{21} \frac{dN_2}{dx} , \qquad (3)$$

$$N_1 + N_2 = 1 , \qquad (4)$$

[6] J. O. Hirschfelder, C. F. Curtiss, and R. B. Bird, Molecular Theory of Gases and Liquids, p 562, Wiley, New York, 1954.

and

$$\dot{\underset{\sim}{n}}_T = \dot{\underset{\sim}{n}}_1 + \dot{\underset{\sim}{n}}_2 \quad . \tag{5}$$

The experimental D_{12} were then normalized to 20°C and 1 atm according to the following relationship.[7]

$$D_{T,P} = D_0\left(\frac{P_0}{P}\right)\left(\frac{T}{T_0}\right)^{1.75} \quad . \tag{6}$$

Experiments with Pure Gases

Ten experiments (near or at uniform pressure) were conducted at room temperature and various mean pressures. Gases which were pure at the point of entrance to the diffusion cell were used in these experiments. The data are tabulated in Table 4. The object of these experiments was to determine D_{12}. See Eqs. (1) and (6).

Experiments with Mixtures

The helium sweep stream was replaced with a He-Ar mixture (69% He–31% Ar), and four uniform total pressure diffusion determinations were made at various mean pressures to verify that Eqs. (1) through (4) are independent of the value of $N_{He}(L)$ and $N_{He}(0)$. The data are presented in Table 5.

Diffusion Superposed on Forced Flow

Low Forced-Flow Rates

Five experiments were performed in which different pressure drops were placed across the septum. The gas sweep streams were pure helium and argon. Each experiment was conducted at an arithmetic mean pressure of 1.97 atmospheres (the arithmetic average took the ΔP into account) and an average temperature of 27.5°C. The results are summarized in Table 6. Since $\dot{n}_{He}$ and $\dot{n}_{Ar}$ are measured directly, as a function of ΔP, as well as of $N_{He}(0)$ and $N_{He}(L)$, Eq. (1) could be used to calculate D_{12} from these data. It should be mentioned that no restrictions have been placed on

[7] A. Lonius, cited by S. Dushman, Scientific Foundations of Vacuum Technique, p 77, Wiley, New York, 1949.

Table 4. Results of Diffusion Experiments Near Uniform Total Pressure

Conditions: Pure sweep gases
Room temperature (29.2°C)

T (°K)	P_m (atm)	N_{He} (x = 0) (mole fraction)	N_{He} (x = L) (mole fraction)	$\dot{n}_{He}$ (moles/sec)	$\dot{n}_{Ar}$ (moles/sec)	$\dot{n}_T$ (moles/sec)	D_{12}* 20°C, 1 atm (cm^2/sec)
				$\times 10^{-5}$	$\times 10^{-5}$	$\times 10^{-5}$	$\times 10^{-3}$
299.2	1.264	0.9948	0.0200	2.319	0.723	1.596	2.443
302.6	1.308	0.9940	0.0169	2.234	0.774	1.460	2.442
304.2	1.360	0.9918	0.0256	2.187	0.792	1.386	2.450
298.2	1.431	0.9936	0.0170	2.317	0.857	1.460	2.624
308.2	1.501	0.9930	0.0206	2.229	0.837	1.392	2.483
304.8	1.929	0.9892	0.0242	2.238	0.812	1.426	2.509
297.2	2.439	0.9925	0.0170	2.402	0.941	1.461	2.798
305.2	3.105	0.9930	0.0220	2.504	0.711	1.792	2.519
301.4	4.904	0.9950	0.0132	1.870	0.752	1.118	2.165
302.7	4.953	0.9936	0.0142	1.861	0.818	1.043	2.240

*Normalized to 20°C and 1 atm by the relationship $D = D_0(P_0/P)(T/T_0)^{1.75}$.

Table 5. Results of Diffusion Experiments Near Uniform Total Pressure Mixtures on Helium Side

T (°K)	P_m (atm)	N_{He} (x = 0) (mole fraction)	N_{He} (x = L) (mole fraction)	$\dot{n}_{He}$ (moles/sec)	$\dot{n}_{Ar}$ (moles/sec)	$\dot{n}_T$ (moles/sec)	D_{12}* 20°C, 1 atm (cm^2/sec)
				$\times 10^{-5}$	$\times 10^{-5}$	$\times 10^{-5}$	$\times 10^{-3}$
301.8	1.277	0.6852	0.0254	1.49	−0.13	1.62	2.078
301.6	1.539	0.6725	0.0472	1.52	0.21	1.31	2.636
305.2	1.952	0.6812	0.0248	1.37	0.21	1.16	2.362
305.7	2.441	0.6823	0.0182	1.34	0.62	0.72	2.717

*Normalized to 20°C and 1 atm by the relationship $D = D_0(P_0/P)(T/T_0)^{1.75}$.

Table 6. Results of Experiments with Diffusion Superposed on Forced Flow

Conditions: Pure sweep gases
Total mean pressure, av 1.97 atm
Room temperature (27.5°C)

$P_{He}-P_{Ar}$ (atm)	P_m (atm)	N_{He} (x = 0) (mole fraction)	H_{He} (x = L) (mole fraction)	$\dot{n}_{He}$ (moles/sec)	$\dot{n}_{Ar}$ (moles/sec)	$\dot{n}_T$ (moles/sec)	D_{12}* 20°C, 1 atm (cm^2/sec)
$\times 10^{-3}$				$\times 10^{-5}$	$\times 10^{-5}$	$\times 10^{-5}$	$\times 10^{-3}$
2.353	1.953	0.9968	0.0314	3.684	−0.418	3.266	2.658
0.040	1.929	0.9892	0.0242	2.238	−0.812	1.426	2.509
−1.338	1.976	0.9886	0.0144	1.976	−1.134	0.842	2.680
−2.548	1.976	0.9888	0.0116	1.579	−1.567	0.012	2.651
−3.488	2.023	0.9854	0.0100	1.498	−1.886	−0.388	2.861
−5.203	1.967	0.9817	0.0083	1.018	−2.202	−1.184	2.616

*Normalized to 20°C and 1 atm by the relationship $D = D_0(P_0/P)(T/T_0)^{1.75}$.

Eq. (1) regarding the causes of $\dot{n}_T$; all that is required is a value for $\dot{n}_T$. This value was obtained from the data through Eq. (5). These experiments were repeated employing the mixture (69% He–31% Ar). The tabulated data are shown in Table 7.

The objectives of this set of experiments were to compare the experimental values of $\dot{n}_{He}$, $\dot{n}_{Ar}$, and $\dot{n}_T$ with the predicted values and to establish that D_{12} could be determined through Eq. (1) regardless of the value of $\dot{n}_T$.

High Forced-Flow Rates

Two series of high forced-flow experiments were performed in which the helium content in the effluent argon sweep stream was carefully controlled at 90% and 80%, respectively. In addition, an arithmetic mean pressure of two atmospheres was rigidly maintained in each determination. To maintain a given concentration, a continuous helium analysis in the argon sweep stream was required. This was accomplished by using a thermal conductivity cell.

Helium was introduced into the system, as in previous diffusion experiments;[4] a portion was forced through the graphite so that relatively large amounts of helium were contained in both gas streams. Through this procedure suitable flow rates were established as well as the desired ΔP and total mean pressure.

To initiate an experiment of this type, a small amount of argon was admitted to one of the sweep streams. This step required a corresponding adjustment in the helium input and output on the other side of the septum to maintain the selected ΔP, flow rates, and total mean pressure. Continual adjustments were made at the inlet and outlet of both sweep streams until the desired gas concentration, ΔP across the graphite, and the arithmetic mean pressure were obtained. The results of these experiments are shown in Tables 8 and 9. These experiments were performed to ascertain the validity of Eqs. (1–5) for high-forced-flow rates.

Table 7. Results of Experiments with Diffusion Superposed on Forced Flow

Conditions: Mixtures
Total mean pressure, av 1.961 atm
Room temperature (26.7°C)

$P_{He}-P_{Ar}$ (atm)	P_m (atm)	N_{He} (x = 0) (mole fraction)	N_{He} (x = L) (mole fraction)	$\dot{n}_{He}$ (moles/sec)	$\dot{n}_{Ar}$ (moles/sec)	$\dot{n}_T$ (moles/sec)
$\times 10^{-3}$				$\times 10^{-5}$	$\times 10^{-5}$	$\times 10^{-5}$
40.56	1.980	0.6896	0.1098	15.43	6.23	21.66
20.75	1.978	0.6876	0.0689	10.33	3.50	13.83
0.56	1.952	0.6875	0.0124	1.37	−0.25	−1.12
−2.99	1.966	0.6814	0.0055	0.776	−2.19	−1.41
−5.803	1.964	0.6764	0.00338	0.48	−2.33	−1.85
−10.26	1.964	0.6688	0.00093	0.131	−5.12	−4.99
−18.33	1.966	0.6466	0.00048	0.068	−9.88	−9.81

Table 8. Results of High-Forced-Flow Diffusion Experiments

Conditions: Total mean pressure, 2.000 atm
Room temperature (24.3°C)
Average argon contamination in argon sweep stream, 40.45%

ΔP (atm)	Argon Side			Helium Side			$\dot{n}_T$ (moles/sec)
	% He	% Ar	$\dot{n}_{He}$ (moles/sec)	% He	% Ar	$\dot{n}_{Ar}$ (moles/sec)	
$\times 10^{-3}$			$\times 10^{-5}$			$\times 10^{-8}$	$\times 10^{-5}$
58.484	79.60	20.40	40.747	99.9724	0.0276	−5.802	40.741
38.30	79.75	20.25	25.592	99.998	0.002	−1.06	3.208
32.071	79.99	20.01	21.557	99.994	0.006	−2.869	2.693
25.543	80.05	19.95	17.259	99.9856	0.0144	−6.679	17.252
19.087	79.15	20.85	10.693	99.9863	0.0137	−5.284	10.688
12.483	79.69	20.31	9.395	99.9889	0.0111	−3.609	9.391
6.049	80.50	19.50	4.750	99.979	0.0210	−20.78	4.729

Table 9. Results of High-Forced-Flow Diffusion Experiments

Conditions: Total mean pressure, 2,000 atm
Room temperature
Average argon concentration in argon sweep stream, 25.71%

ΔP (atm)	Argon Side			Helium Side			$\dot{n}_T$ (moles/sec)
	% Ar	% He	$\dot{n}_{He}$ (moles/sec)	% He	% Ar	$\dot{n}_{Ar}$ (moles/sec)	
$\times 10^{-3}$			$\times 10^{-5}$				$\times 10^{-5}$
28.961	89.62	10.38	25.601	99.996	0.0042	-1.467×10^{-8}	25.600
18.787	89.93	10.07	17.390	99.976	0.0242	-9.131×10^{-8}	17.381
8.677	90.27	9.73	8.688	99.987	0.0128	-3.763×10^{-7}	8.650
7.868	89.70	10.30	7.783	99.780	0.220	-7.374×10^{-7}	7.709
5.105	89.72	10.28	5.479	99.813	0.187	-1.647×10^{-6}	5.314
0.504	90.16	9.84	2.937	99.469	0.531	-5.357×10^{-6}	2.401

DISCUSSION

Diffusion Mechanism Near Zero Forced-Flow Rates

The normalized diffusion coefficients near zero forced-flows (using pure gases and mixtures) are plotted vs reciprocal mean pressure on Fig. 2. The horizontal curve of Fig. 2 shows that the flow Eqs. (1) and (6) employed in the AGOT determinations are applicable to these data. At low forced-flow rates, the primary mechanism controlling the interdiffusion of helium and argon was classical mutual diffusion.

Effect of Mixtures at Boundaries

In a previous report[4] dealing with the interdiffusion of pure helium and argon through AGOT graphite, some speculation was given as to what effect changing the composition of the gas stream would have on the value of D_{12}. These experiments were intended to support the previous speculations.

The average normalized mutual diffusion coefficient for the pure gases was 2.47×10^{-3} cm^2/sec compared with an average value of 2.45×10^{-3} cm^2/sec for the known mixture. These results show that D_{12} is not affected; therefore Eq. (1) adequately compensates for the variable concentration at the boundary.

Net Drift at Uniform Total Pressure

Since the D_{12} values obtained in the AGOT experiments at nonuniform total pressure are in excellent agreement with the uniform total pressure results, no special care was taken in these experiments to obtain the net drift relationship for each individual determination. A clear and somewhat striking demonstration of the net drift can be obtained from the superposed data for the pure gases (plotted on Fig. 3) and for the experiments with mixtures (plotted on Fig. 4). On both plots, $\dot{n}_{He}/\dot{n}_{Ar} = 3$ at $\Delta P = 0$. This value is approximately equal to $(M_{Ar}/M_{He})^{\frac{1}{2}}$. Thus the relationship is the same as that in AGOT and does not depend on the concentration of the sweep gases.

The results of recent work which concerns a theoretical derivation of the rate ratio at $\Delta P = 0$ is given in the appendix of this report. The

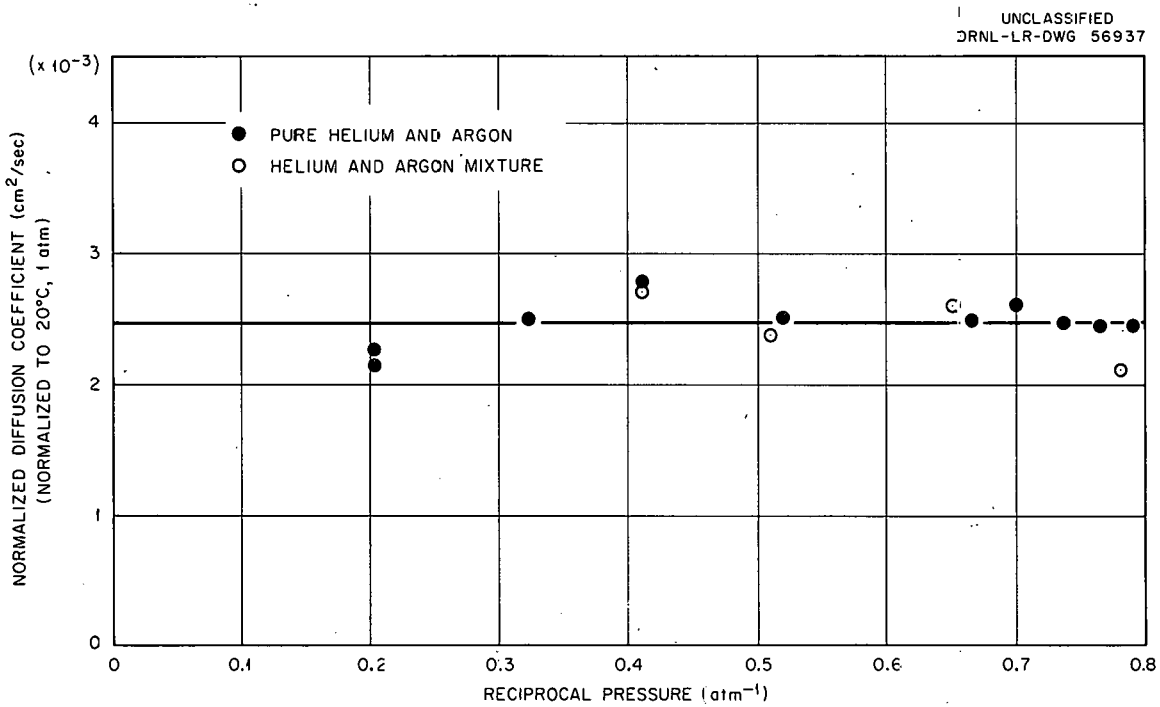

Fig. 2. Mutual Diffusion Coefficient for Helium-Argon in Speer No. 1 Graphite.

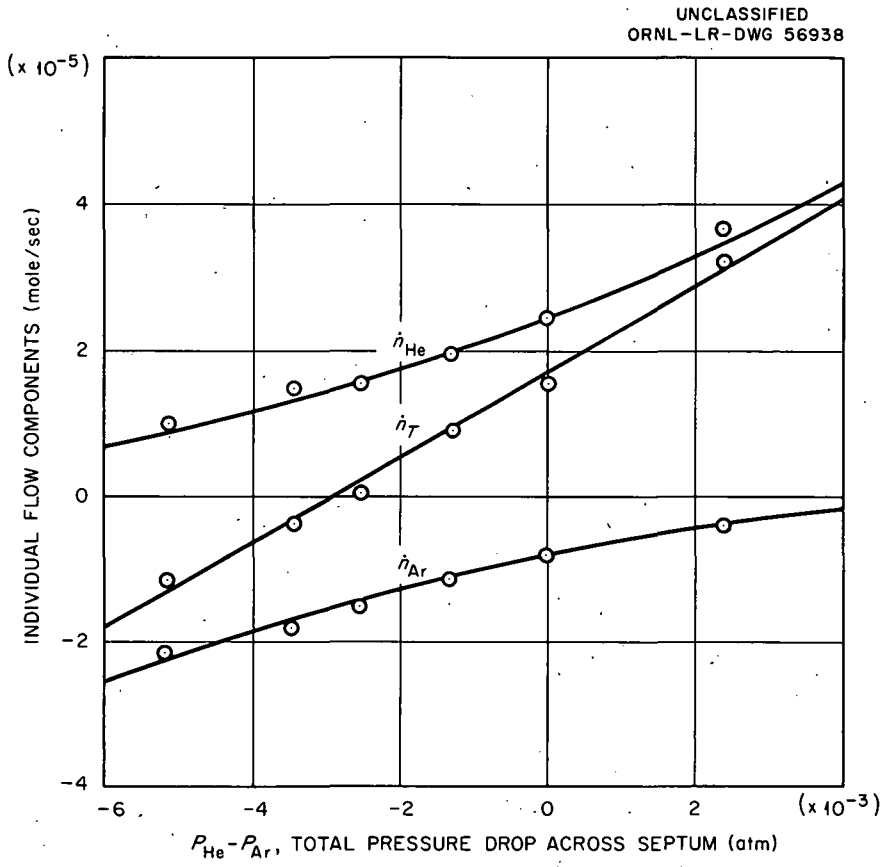

Fig. 3. Results of Diffusion Experiment at Room Temperature and 1.971 atm. Curves are predicted values.

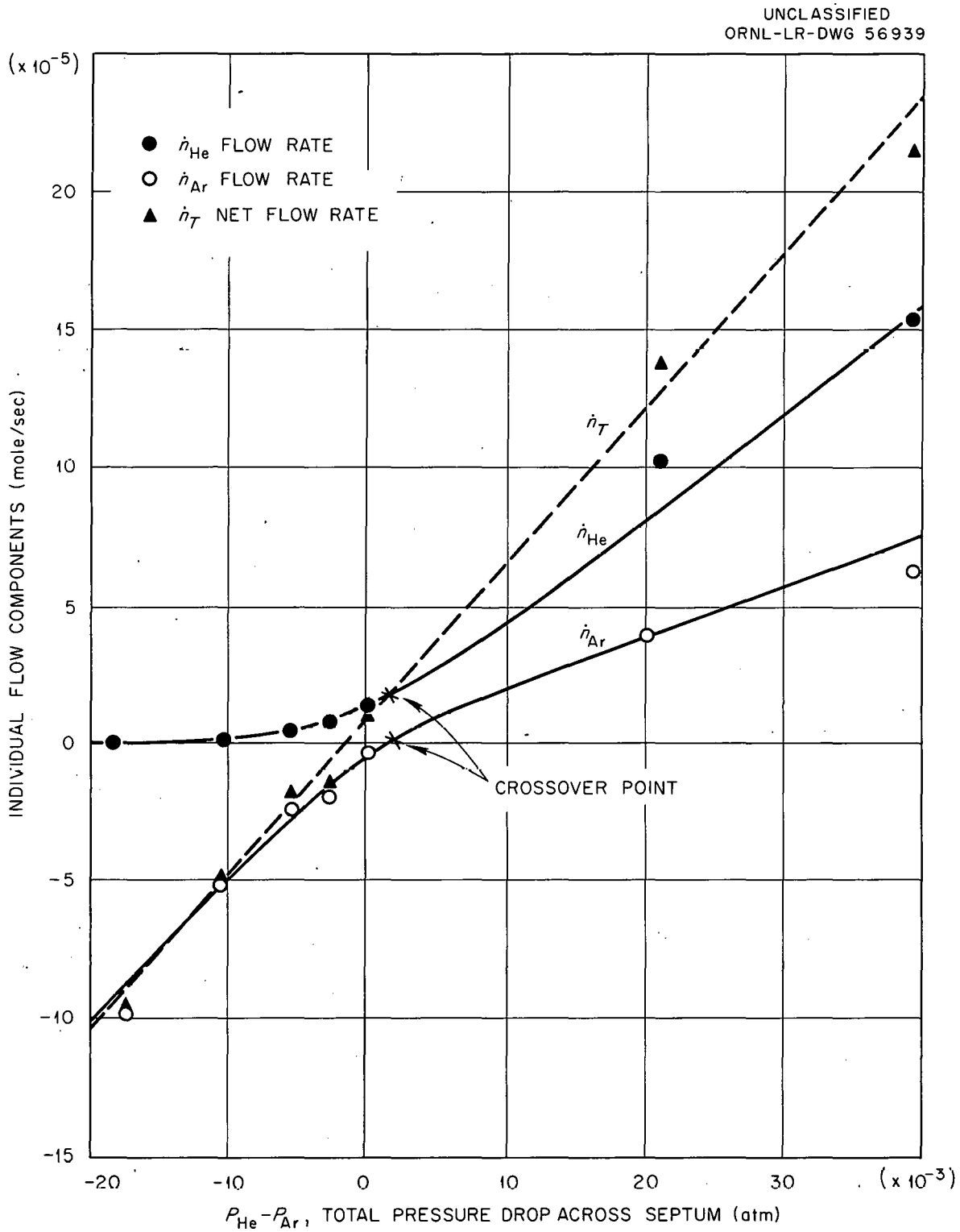

Fig. 4. Results of Diffusion Experiments Employing Helium-Argon Mixture at Room Temperature and 1.967 atm. Curves are predicted values.

readers are urged to review this section, as the derivation adopted by the authors in the AGOT interdiffusion report is incorrect.

Superposed Flow

Although D_{12} remained constant, the individual component flow rates were considerably altered when a ΔP was placed across the graphite. The results of the pure-gases and known-mixture experiments are shown on Figs. 3 and 4, respectively. The curves are the predicted values, while the symbols represent the experimental data. The equation for the net transport when superposed diffusion and forced flow are combined is

$$\underset{\sim}{\dot{n}}_T = \underset{\sim}{\dot{n}}_T' + \underset{\sim}{\dot{n}}_f \ , \qquad (7)$$

where $\dot{n}_T'$ is the superposed flow, $\dot{n}_f$ is the forced flow (calculated through the permeability constant), and $\dot{n}_T$ is the net drift at uniform total pressure.

Comparison between predicted and calculated superposed and forced-flow rates required knowledge of the cell permeability to helium-argon mixtures. The permeability constant, at the conditions of the experiment with various helium-argon mixtures, was estimated through the experimental permeability data and a knowledge of the viscosity (as a function of helium concentration and the radial thickness factor*). A typical example is shown in Fig. 5a. In addition the concentration profile shown in Fig. 5a was also prepared. A combination of the information given in Fig. 5a leads to the plot in Fig. 5b. The area under this curve was taken to be the reciprocal of the average permeability constant. This average would apply to estimates of $\dot{n}_f$ when the gas in the pores exhibited the concentration profile shown in Fig. 5a. This procedure was repeated whenever the concentration profile was markedly altered. Calculated and experimental values show that the estimated superposed-flow patterns are within the limits of the experimental error and the crossover points (where the component rates change sign) were not reached with pure gases. They were, however, observed in experiments with mixtures.

---

*$z = \dfrac{\ln r - \ln r_1}{\ln r_0 - \ln r_1}$ (ref 4).

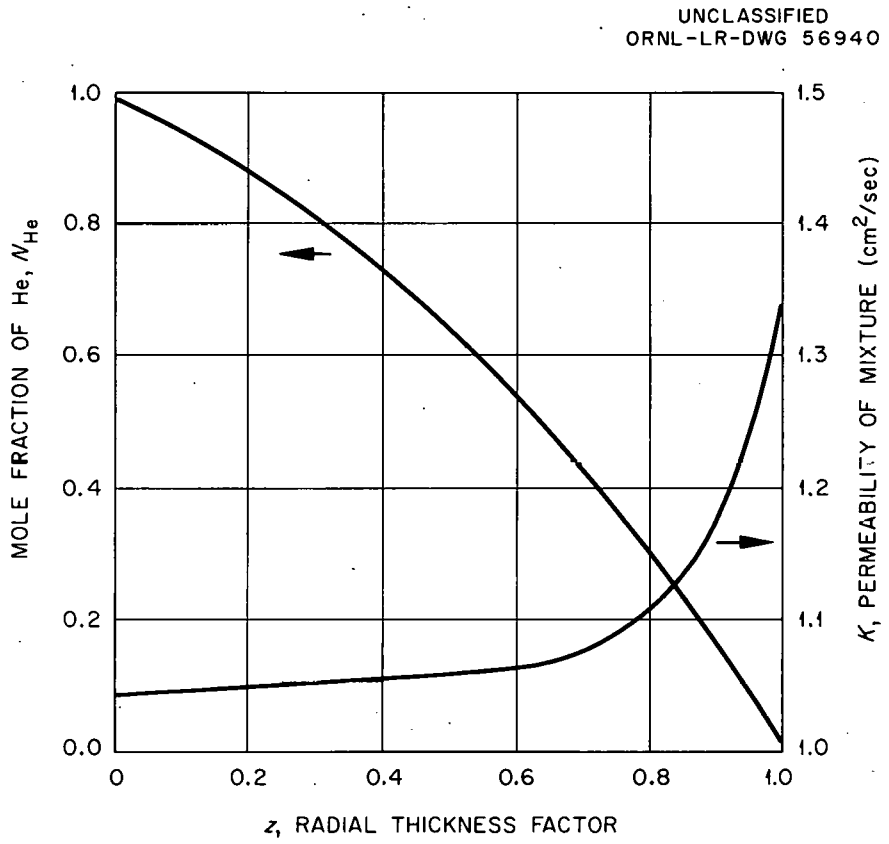

Fig. 5a. Viscosity Ratio and Permeability at 20°C and 2 atm as a Function of Composition.

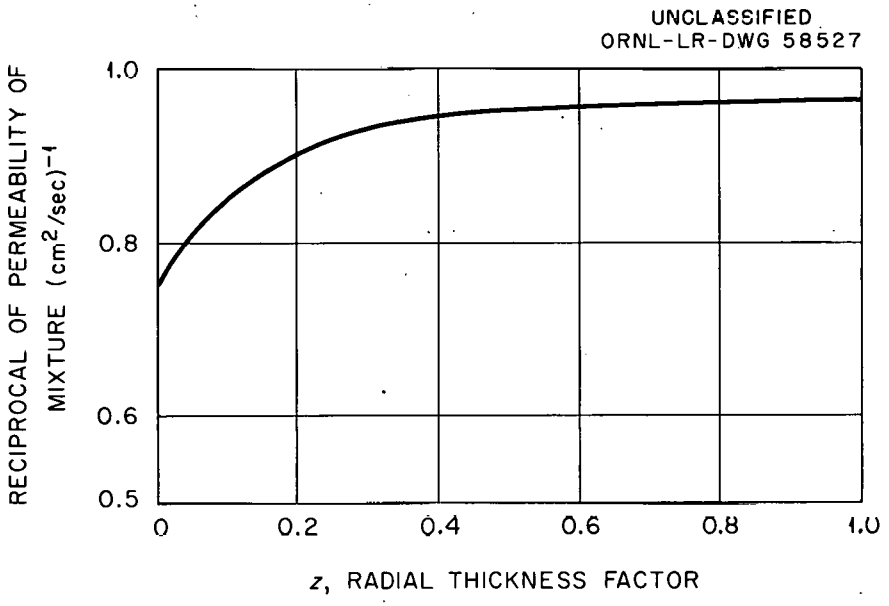

Fig. 5b. Resistance to Flow Versus Position.

Back-Diffusion

Certain assumptions can be made concerning individual component flow rates in high-forced-flow experiments. These assumptions permit considerable rearranging and combining of flow equations into forms which are convenient for graphic presentation. This, in turn, will be helpful in discussing the results.

A combination of Eqs. (1), (4), and (5) leads to

$$\exp\ (\dot{n}_T/B) = \frac{\dot{n}_2 + \dot{n}_T[N_{Ar}(L)]}{\dot{n}_2 + \dot{n}_T[N_{Ar}(0)]}\ , \tag{8}$$

where $B = D_{12}(A/L)(P/RT)$.

Since $N_{Ar}(0) \cong 0$ under the conditions of these experiments Eq. (8) can be rearranged to give

$$\frac{\dot{n}_2}{\dot{n}_T} = \frac{N_{Ar}(L)}{\exp\ (\dot{n}_T/B) - 1} \cong N_{Ar}(L)\ \exp\ (-\dot{n}_T/B)\ , \tag{9a}$$

which is also

$$\ln \frac{\dot{n}_{Ar}}{\dot{n}_T N_{Ar}(L)} = -\frac{\dot{n}_T}{B}\ . \tag{9b}$$

At high sweep rates $\dot{n}_T = \dot{n}_{He} \cong \dot{n}_f$. Thus,

$$\ln \frac{\dot{n}_{Ar}}{\dot{n}_{He}} - \ln N_{Ar}(L) \cong -\frac{N_{Ar}(L)\dot{n}_f}{B} = -\frac{N_{Ar}(L)KA\ \Delta P}{LB} = -\frac{K}{D_{12}}\frac{\Delta P}{P}\ . \tag{9c}$$

If one takes an approximate pressure diffusion term into account, it can be shown in a similar manner that,[8]

$$\ln \frac{\dot{n}_{Ar}}{\dot{n}_{He}} - \ln N_{Ar}(L) \cong -\left(\frac{K}{D_{12}} - 8.98\right)\frac{\Delta P}{P}\ . \tag{10}$$

---

[8] H. L. Weissberg and A. S. Berman, Diffusion of Radioactive Gases Through Power Reactor Graphite, ORGDP-KL-413 (Apr. 6, 1959).

A plot of these data in terms of Eq. (9c) is shown on Fig. 6. Above a ΔP of about 12×10^{-3} atm across the septum, the experimental data on component flow rates begin to deviate from the predicted curve, which is related to Eq. (9a). This deviation becomes appreciable as the flow rate is increased. For example, at a $\Delta P = 38.3 \times 10^{-3}$ atm, the predicted value

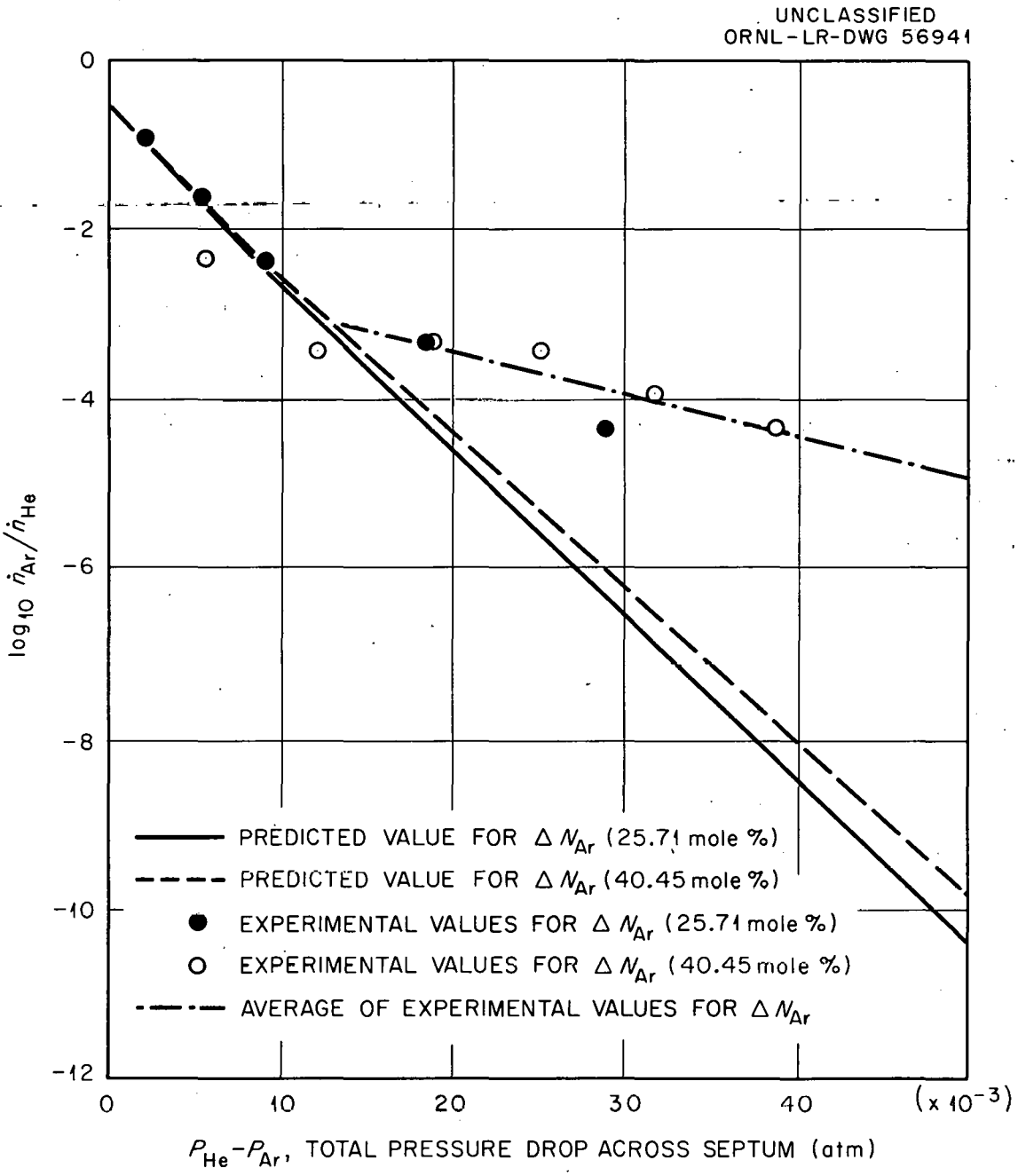

Fig. 6. Comparison of Predicted and Experimental Values at High Helium Sweep Rates.

for $\dot{n}_{Ar}$ is 5.26×10^{-12} mole/sec as compared with an experimental value of 1.08×10^{-8} mole/sec.

At low sweep rates (small ΔP) near uniform pressure, the diffusion occurs mainly in the largest passages. The small amount which might diffuse through the smallest pores is negligible. On the other hand, high sweep rates, which are selective toward the largest pores, blank out the diffusion contribution of the largest holes, leaving only the diffusion contribution of the smallest pores, which were undetectable (as a result of the small value) in previous experiments.

The next point of interest involves the mechanism of the small-passage contributions to the diffusive process.

Pressure diffusion calculations based on Eq. (10) show only a very slight increase in the $\dot{n}_{Ar}$ flow rate over the predicted value. This eliminates the possibility of pressure diffusion.

Additional information is gained by plotting the data as shown on Fig. 7. The ordinate of this curve is log $\dot{n}_{Ar}/N_{Ar}P_m$ which would also be log $D_{K_{Ar}}/RTL$ where D_K is the Knudsen diffusion coefficient. The results shown should be the same for both experiments (since different driving forces are taken into account) and should become independent of sweep rates at higher values of sweep rates. This information is demonstrated in Fig. 7.

We conclude that the contribution of the small pores follows a Knudsen diffusion mechanism with a D_K of 5.68×10^{-6} cm^2/sec. Furthermore, the results clearly show that back diffusion cannot be completely suppressed by high helium sweeps either in Knudsen materials (one could predict this by theory) or in large-pore graphites.

This leads to another conclusion: that a critical sweep rate was obtained for this particular grade of graphite. For example, the critical sweep rate on Fig. 7 is 25×10^{-5} mole/sec. If the sweep rate is decreased below this value the contamination will increase, whereas sweep greater than this value would require larger reprocessing capacities without additional decrease in contamination.

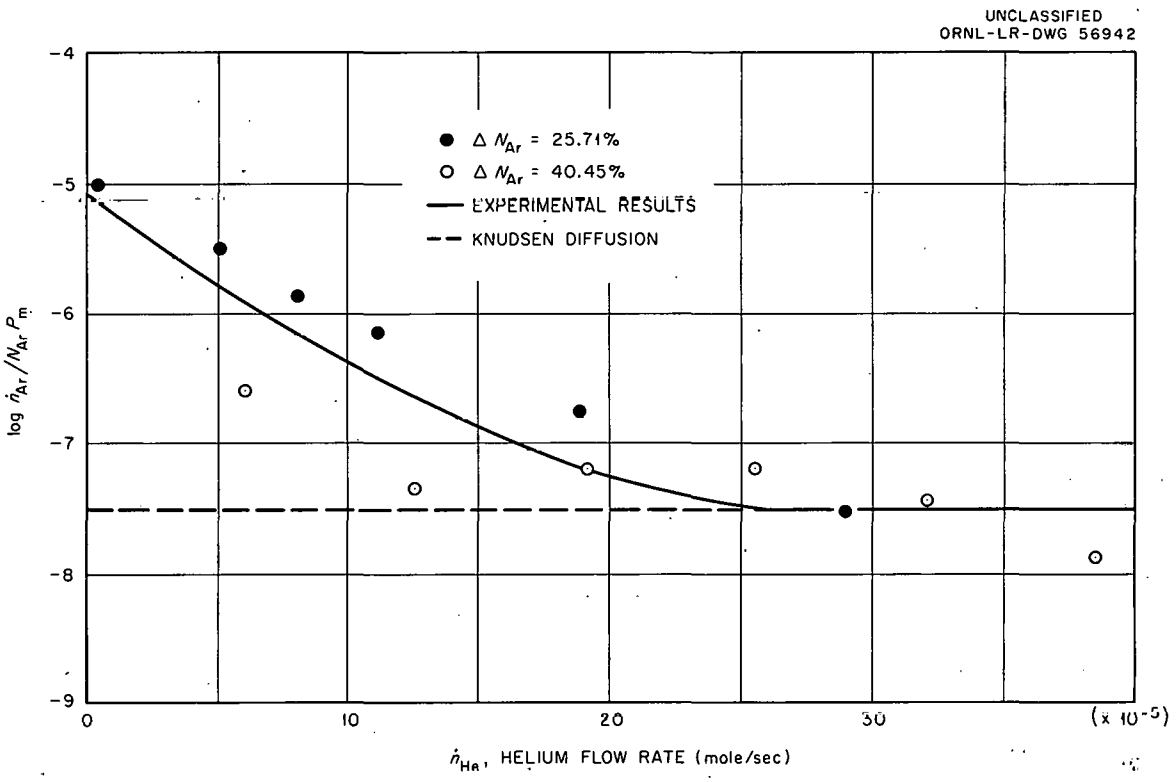

Fig. 7. Back Diffusion Behavior of Argon in Speer Graphite at Room Temperature and 2.000 atm at High Helium Sweep Rates.

CONCLUSIONS

1. At low forced-flow rates, the primary mechanism controlling the interdiffusion of helium and argon was classical mutual diffusion.

2. The flow equations employed in AGOT determinations are applicable to these data.

3. A net drift was obtained, in which the ratio of the helium diffusion rate to that of argon was inversely proportional to the ratio of the square roots of the atomic weights of the two gases.

4. As a result of experiments utilizing mixtures, crossover points were observed, but their significance has not yet been explained.

5. Flow equations employed at low forced-flow rates are invalid under conditions of high forced-flow rates.

6. Pressure diffusion played no significant role in the diffusion mechanism at high forced-flow rates.

7. Experiments at high-forced-flow rates show that the contribution of the small pores follows a Knudsen diffusion mechanism.

8. A critical sweep rate was obtained for the grade of graphite studied. If the sweep rate is decreased below this value the contamination will increase, whereas sweep rates greater than this value would require large reprocessing capacities without additional decrease in contamination.

APPENDIX

A Diffusion Model for Large-Pore Graphites

E. A. Mason R. B. Evans III

In the previous report,[4] which dealt with AGOT graphite, the inverse relation between square roots of the atomic weights and the diffusion rates of the gases was developed on two compensating errors. These were:

1. the incorrect assumption that the net forces on the septum were zero when $\nabla P = 0$,
2. the incorrect calculation of momentum transfer [see Eq. (13) in ref 4].

In the process of explaining this phenomenon correctly a unique diffusion model applicable to porous media has been suggested.

The reader may recall that the experimental diffusion rates are based on steady-state measurements of the effluent rates and compositions of the sweep streams.[9] This discussion concerns experiments wherein the total pressure and temperature on each side of the septum are held equal. The diffusion rate, J_i (particles/cm^2·sec), of each gas is constant at any point along the flow path.

The ultimate goal is an equation of the form:[10,11]

$$\underset{\sim}{J}_i = -D_{i,\text{eff}} \nabla n_i + \delta x_i \underset{\sim}{J} , \quad \left[\begin{array}{l}\delta = 0, \text{ flow is Knudsen} \\ \delta = 1, \text{ diffusion is classical}\end{array}\right], \qquad (1)$$

where

J = the net flux* or $\sum_{i=1}^{\nu} \underset{\sim}{J}_i$, particles/cm^2·sec,

$D_{i,\text{eff}}$ = the apparent diffusion coefficient, cm^2/sec,

n_i = the particle density of the i^{th} component,

n = the total density or $\sum_{i=1}^{\nu} n_i$ (particles/cm^3),

x_i = the particle fraction of the i^{th} component.

Equation (1) is a series resistance formula and is an accepted relationship for diffusion of binary mixtures when $\delta = 1$. The variable, δ, is defined over the interval $0 < \delta < 1$; δ increases as the ratio of the average pore radius to the mean free path (a/λ) increases. When flow is Knudsen, $\delta x_i \underset{\sim}{J} = 0$. Furthermore, $\nabla n_1 = -\nabla n_2$ (for a binary mixture) when $P = 0$. The well-known results:

$$\underset{\sim}{J}_1/\underset{\sim}{J}_2 = -D_{1,\text{eff}}/D_{2,\text{eff}} = -(m_2/m_1)^{\frac{1}{2}} , \qquad (2a)$$

---

[9] E. Wicke and R. Kallenback, Kolloid-Z. 97, 135 (1941).

[10] R. D. Present, Kinetic Theory of Gases, p 49, McGraw-Hill, New York, 1958.

[11] J. O. Hirschfelder, C. F. Curtiss, and R. B. Bird, Molecular Theory of Gases and Liquids, p 519, Wiley, New York, 1954.

*$A\underset{\sim}{J}_i = \dot{n}_i N$, where A (cm^2) is the area normal to flow and N is Avogadro's number. The flow is expressed in terms of $\underset{\sim}{\dot{n}}_i$ in Fig. 1, p 12, ref 4.

and

$$\underset{\sim}{J} = \underset{\sim}{J}_1[1 - (m_1/m_2)^{\frac{1}{2}}] = \underset{\sim}{J}_2[1 - (m_2/m_1)^{\frac{1}{2}}] \qquad (2b)$$

follow by the previous definitions.

The present discussion deals primarily with similar relationships under the same conditions when $\delta \rightarrow 1$. An important clue is offered by the treatments of Epstein[12] and Waldmann[13] of the interdiffusion of a ternary system composed of two gases and a dust suspension. Since the dust was successfully treated as being a third gas component in previous work, the same approach is followed with respect to the interdiffusion of a binary mixture in a porous medium. The graphite is visualized as being a large number of carbon particles suspended in the diffusion path. The particles are subject to forces which tend to cause them to move; however, they are fixed ($\underset{\sim}{J}_d = 0$) and exhibit a concentration profile which is constant with position ($\nabla x_d = 0$). A combination of these conditions, Waldmann's[13] expression for D_{id}, (where $m_d \gg m_i$ and the radii, r, are such that $r_d \gg r_i$), and suitable diffusion equations (see Hirschfelder's Eq. 8.1-3) leads to the expression:

$$\sum_{\substack{i \\ i \neq d}} J_i \, (m_i)^{\frac{1}{2}} \left(1 + \frac{\pi}{8} \alpha_i\right) = 0 \; . \qquad (3)$$

The subscript i refers to the two gases; subscript d refers to the carbon dust particles. When the accommodation coefficients, α_i, of the two gases are equal, Eqs. (3) and (2a) are identical. This is somewhat surprising because no direct restrictions regarding a/λ or δ were applied to derive Eq. (3) except those mentioned in connection with m_d and r_d.

Other investigators[4,14,15,16] have developed Eq. (2a) (for $\delta \rightarrow 1$) using the incorrect premise that the net force on the graphite septum is

---

[12] P. S. Epstein, Phys. Rev. 23, 710 (1924).
[13] L. Waldmann, Z. Naturforsch. 14a, 589 (1959).
[14] J. Hoogschagen, J. Chem. Phys. 21, 2096 (1953).
[15] E. Wicke, private communication (November 1960).
[16] H. A. Kramers and J. Kistemaker, Physica 10, 699 (1943).

zero since $\nabla P = 0$. The latter is merely a condition that Poiseuille flow does not exist. Actually, the cell tends to move under the conditions of the experiment in a manner discussed by Waldmann.[13]

It is apparent from the use of diffusion equations for a ternary mixture in the derivation of Eq. (3) that Eq. (1) is merely a phenomenological expression – particularly when $1 > \delta > 0$. Equation 1 is a convenient means of obtaining an integrated rate expression in terms of $D_{i,eff}$. It shall be necessary to define $D_{i,eff}$ and δ in terms of D_{id}, D_{12} and D_{21}. The AGOT data appear to be a limiting case where $\delta \rightarrow 1$ and $D_{1,eff} \rightarrow D_{12} = D_{21}$, the latter being subject to corrections for the internal geometry of the graphites.

THIS PAGE

WAS INTENTIONALLY

LEFT BLANK

ORNL-3117
UC-4 — Chemistry
TID-4500 (16th ed.)

INTERNAL DISTRIBUTION

1. G. M. Adamson
2. L. G. Alexander
3. C. J. Barton
4. S. E. Beall
5. R. J. Beaver
6. M. Bender
7. A. S. Berman
8. D. S. Billington
9. J. P. Blakely
10. F. F. Blankenship
11. E. P. Blizard
12. C. M. Blood
13. A. L. Boch
14. E. G. Bohlmann
15. C. J. Borkowski
16. W. F. Boudreau
17. G. E. Boyd
18. E. J. Breeding
19. J. C. Bresee
20. R. B. Briggs
21. W. E. Browning
22. S. Cantor
23. F. L. Carlsen, Jr.
24. C. E. Center (K-25)
25. R. A. Charpie
26. R. S. Cockreham
27. Esther Cohn
28. T. E. Cole
29. J. H. Coobs
30. J. A. Conlin
31. W. B. Cottrell
32. J. A. Cox
33. F. L. Culler
34. H. N. Culver
35. J. S. Culver
36. J. H. DeVan
37. D. A. Douglas
38. E. P. Epler
39-48. R. B. Evans
49. R. M. Evans
50. J. E. Eorgan
51. D. E. Ferguson
52. J. Foster
53. J. L. Fowler
54. A. P. Fraas
55. J. H. Frye, Jr.
56. C. H. Gabbard
57. A. E. Goldman
58. B. L. Greenstreet
59. W. R. Grimes
60. E. Guth
61. J. P. Hammond
62. W. O. Harms
63. T. Hikido
64. M. R. Hill
65. E. E. Hoffman
66. H. W. Hoffman
67. A. Hollaender
68. A. S. Householder
69. H. Inouye
70. R. G. Jordan (Y-12)
71. W. H. Jordan
72. P. R. Kasten
73. G. W. Keilholtz
74. C. P. Keim
75. M. T. Kelley
76. J. J. Keyes
77. B. W. Kinyon
78. R. B. Korsmeyer
79. P. Lafyatis
80. J. A. Lane
81. S. C. Lind
82. R. S. Livingston
83. H. G. MacPherson
84. W. D. Manly
85. E. R. Mann
86. R. W. McClung
87. H. E. McCoy
88. H. C. McCurdy
89. W. B. McDonald
90. H. F. McDuffie
91. D. L. McElroy
92. C. J. McHargue
93. F. R. McQuilkin
94. H. J. Metz
95. A. J. Miller
96. R. S. Miller
97. J. G. Morgan
98. K. Z. Morgan
99. F. H. Neill
100. M. L. Nelson
101. L. G. Overholser

102. N. Ozisik
103. P. Patriarca
104. B. R. Pearson (Y-12)
105. A. M. Perry
106. D. Phillips
107. C. A. Preskitt
108. W. T. Rainey
109. M. E. Ramsey
110. P. M. Reyling
111. T. K. Roche
112. M. W. Rosenthal
113. A. F. Rupp
114. G. Samuels
115. H. W. Savage
116. A. W. Savolainen
117. J. L. Scott
118. C. H. Secoy
119. O. Sisman
120. E. D. Shipley
121. M. J. Skinner
122. G. M. Slaughter
123. N. V. Smith
124. A. H. Snell
125. B. A. Soldano
126. I. Spiewak
127. E. Storto
128. R. A. Strehlow
129. R. D. Stulting
130. J. C. Suddath
131. C. D. Susano
132. J. A. Swartout
133. A. Taboada
134. E. H. Taylor
135. D. F. Toner
136. W. C. Thurber
137. D. B. Trauger
138-147. J. Truitt
148. C. S. Walker
149. J. L. Wantland
150-159. G. M. Watson
160. A. M. Weinberg
161. J. R. Weir
162. H. L. Weissberg (K-25)
163. M. E. Whatley
164. J. C. White
165. E. A. Wick
166. G. C. Williams
167. C. E. Winters
168. J. Zasler
169. P. H. Emmet (consultant)
170. E. A. Mason (consultant)
171. F. T. Miles (consultant)
172. F. T. Gucker (consultant)
173. J. W. Prados (consultant)
174. F. Daniels (consultant)
175. ORNL - Y-12 Technical Library, Document Reference Section
176-177. Central Research Library
178. Laboratory Records, ORNL R.C.
179-198. Laboratory Records Department

EXTERNAL DISTRIBUTION

199. L. Brewer, University of California
200. R. H. Condit, University of California
201. F. T. Salzano, Brookhaven National Laboratory
202. P. L. Walker, Jr., Pennsylvania State University
203. Division of Research and Development, AEC, Washington
204. Division of Research and Development, AEC, ORO
205. Division of Reactor Development, AEC, Washington
206. Division of Reactor Development, AEC, ORO
207-209. W. F. Banks, Allis-Chalmers Mfg. Co.
210-212. P. D. Bush, Kaiser Engineers
213. E. Creutz, General Atomic
214. D. H. Fax, Westinghouse Atomic Power Division
215-217. R. B. Duffield, General Atomic
218. T. Jarvis, Ford Instrument Co.
219. Richard Kirkpatrick, AEC, Washington
220-221. H. Lichtenburger, General Nuclear Engineering Corp.
222. J. P. McGee, Bureau of Mines, Appalachian Experiment Station

223. S. G. Nordlinger, AEC, Washington
224. H. B. Rahner, Savannah River Operations Office
225. Corwin Rickard, General Atomic
226. S. T. Robinson, Sanderson and Porter
227. M. T. Simnad, General Atomic
228. Donald Stewart, AEC, Washington
229. G. W. Tompkin, Mallinckrodt Nuclear Corporation
230. Philip L. Walker, Pennsylvania State University
231. R. E. Watt, Los Alamos Scientific Laboratory
232-233. W. L. Webb, East Central Nuclear Group, Inc.
234-750. Given distribution as shown in TID-4500 (16th ed.) under Chemistry category